Jurnal Kejuruteraan 35(5) 2023: 1165-1179
https://doi.org/10.17576/jkukm-2023-35(5)-17

An Analysis of The Effect of Heterogeneously Distributed Inertia Constant in Generation Mix Power System by Using the Graph Theory and Dijkstra's Algorithm

Harshada Nerkar*, Prasanta Kundu & Anandita Chowdhury

Department of Electrical Engineering,

Sardar Vallabhbhai National Institute of Technology, Gujrat, India

**Corresponding author: harshadanerkar22@gmail.com; ds17el002@svnit.ac.in*

Received 3 February 2023, Received in revised form 20 March 2023
Accepted 20 April 2023, Available online 30 September 2023

ABSTRACT

A modern power system with a generation mix of conventional and renewable energy sources (RES) creates stability issues. This requires a detailed analysis of the system with an exact share of active power through the generating sources according to nature, location, and control. The interconnected network with a large number of rotating machines at the generation side works coherently with each other. As the share of RES increases, it leads to reduce rotational inertia in the power system. The most important factor affected by inertia is the rate of change of frequency (RoCoF). The higher RoCoF leads the system more vulnerable to small disturbances in the power system. In a large power system network with numerous generating sources and transmission lines, it is difficult to determine the availability of inertia in the system. This paper incorporates the concept of graph theory in the IEEE 30 bus system to analyze the impact of heterogenous inertia distribution on frequency stability. The graph theory network gives the idea about the distance between the nodes and it is helpful to find the share of power from the generating sources. In this paper, we calculate the shortest path between the nodes or substations by using Dijkstra's algorithm. The betweenness centrality of the node detects the vulnerable nodes in the system from the frequency response point of view.

Keywords: Renewable energy sources; inertia constant; rate of change of frequency; Graph theory; Dijkstra's Algorithm

INTRODUCTION

MOTIVATION

The worldwide share of renewable energy sources (RES) in the power system networks increases as a shortage of conventional resources like fossil fuels (Harun et al. 2022).

Future power systems with generation mixes of conventional and non-conventional energy sources such as Thermal, Hydro, Nuclear, biomass, wind, solar, etc (Basri et al. 2021). The RESs have different generation and operational characteristics than conventional energy sources. These RESs are intermittent in nature and feed power into the system through power electronic devices. Due to the absence of rotating parts in the RES generation system, we can call them non-synchronous generators. These non-synchronous generators do not contain inertia, while the addition of RES in the existing network reduces the overall inertia of the system. The low inertia power networks are responsible for high RoCoF and result in maximum frequency nadir during power system operation and this may lead to cascade failure in contingency events. Frequency nadir is an important metric for the power system operator to respond to the step change in load or generation side. In this paper, the impact of the share of RES on RoCoF and frequency nadir is discussed in detail on IEEE 30 bus system.

The power generation mixes vary from one to another country according to local resource availability, national policies, and global markets. Indian power grid frequency is 50Hz and a permissible band of frequency range is between 49.5 Hz -50.2 Hz according to Indian Electricity Grid Code (IEGC).

India is committed to achieving a 40% share of RES generation by 2030, while considering the significant growth in renewable energy the Power System Operation and Control (POSOCO) explores the inertia estimation for the Indian power grid (POSOCO and IITB 2022).

LITERATURE SURVEY

Inertia is a needful property of a moving system that depends on the energy stored in the wheel of a bicycle or the rotor of synchronous generators. The presence of inertia allows the bicycle to be in motion without pedaling for some time. Similarly in the case of a synchronous grid comprise of generators rotating with the same frequency, the presence of an inertia constant prevents the system from unstable operation during disturbance for a few seconds (Denholm et al. 2020). The large and complex network of power systems comprised of various generating sources has heterogeneous inertia constant (Nouti et al. 2021). The power system inertia constant is determined as the time required for the synchronous generators to respond to the deviation in system frequency. The power frequency deviation depends on the generation and demand imbalance. The conventional energy sources in the power system feed power through synchronous generators which are worked coherently. The synchronization during the operation of the power system is smooth due to the similar topology of the connected generators. It is difficult to synchronize conventional generating sources with RES because of different generation characteristics. Due to the stochastic nature of the RES, the inertia constant will become a time-varying quantity (Makolo et al. 2021). During disturbances in the power system, the converter-based generators are unable to ride through for a few seconds also. The system with low inertia constant has a higher Rate of Change of Frequency (RoCoF) which increases the vulnerability to disturbances in the power system (Entsoe 2020). The RoCoF is based on the variation of inertia constant in a power system with RES and dependent on the generation patterns and load demand (Wilson et al. 2019), (Prabhakar et al. 2022). The rate of change of frequency is measured by the difference between two successive frequency values concerning time (Pentayya et al. 2012). The analysis of the percentage-wise share of the RES in the power system gives the idea about the minimum requirement of inertia according to system frequency nadir and RoCoF value during the contingency event (Nerkar et al. 2023). The virtual inertial power is fed by various control topologies to mitigate this deficit of inertial power in low inertia systems (Nerkar et al. 2021), (Kerdphol et al. 2018),(Mandal et al. 2021). The exact detection of the power system frequency is necessary to estimate the spatial-temporal inertia value for the compensation of the lack of inertia value in a particular area/zone (Tan et al. 2022),(Phurailatpam et al. 2021),(Su, Y et al. 2020),(Rezkalla et al. 2018). In the case study of Rwanda's power system, the author estimates the inertia value for the different scenarios and it justifies the rise in share of RES lowers the system inertia and requirement to enhance the frequency regulation technique (Mudaheranwa et al.2022). The frequency detection at the local level determines the active power deficit at a particular point and it is easy to take corrective action (Azizi et al. 2020). The rating of the generators also affects the inertia constant of the system, the generators with lower ratings have higher inertia constant as compared to high-rated generators (Qaid et al. 2021). To keep the system balance throughout the operation of the power system, it is necessary to maintain the required system inertia (Wu et al. 2021). It is essential to know the minimum inertia value of the particular power system for further addition of the RES in the existing network (Mehigan et al. 2020). It is difficult to determine the inertia constant in a large and complex network with mixed generations. It is dependent on the stored kinetic energy in the rotor of the machine and the time taken to respond to the changes in the synchronous power system (Rampokanyo et al. 2019). To study the large network of power system with high number of transmission lines and spatially distributed generators and load, the spectral graph theory approach is utilized for the analysis purpose (Retiére et al. 2019), (Dwivedi et al. 2009). The Laplacian matrices are derived from the graph theory of network for the stability analysis of inverter connected microgrids (Iyer et al. 2010),

(Garg et al. 2006). The graph theoretical methodology is developed for selecting the suitability index of the power plant by forming attribute matrices of the system (Garg et al. 2006). In a mixed-generation system, the location of low inertia areas affects the dynamics of the power system (Tamrakar, et al. 2017),(Alahmad et al. 2021). The inertial index terminology is introduced by (Brahma et al. 2021), which determines the locational capability of the system to resist a frequency changes. Organization paper, focuses on the impact of mixed generation on power system frequency response in IEEE 30 bus system. This is achieved by implementing the Dijkstra's pathfinding algorithm on graph theory of 30-bus system to find the distance between the buses with low inertia bus for further action.

ORGANIZATION OF PAPER

Section 1 is comprised of the motivation for the research work and the respective literature survey. The problem identification is implemented on IEEE 30 bus system by

using MATLAB software and is described in section 2. Section 3 gives the idea of Dijkstra's pathfinding algorithm and its implementation in graph theory of 30 bus system. The node centrality and its analysis are elaborated in section 4, to check the vulnerable nodes in 30- bus system with heterogenous inertia constant. The verification of this approach is analyzed at disturbance conditions in the power system in section 5.

BACKGROUND

An electrical power system is a large and complex network comprised of generators, busbars, transmission lines, etc. For analysis purposes, the power system network is converted into graph theory. The IEEE standard 30 bus system (Shahidehpour et al. 2004), shown in figure 1 is considered for further analysis of the effect of inertia constant variation through the graph theory approach. In IEEE 30 - bus system there are 30 vertices and 41 edges in the graph as shown in figure 2, the blue spheres are buses and red one denotes the generator connected to the spheres. The vertices or node represents the bus number and edges are depicting the connection between two vertices i.e., transmission lines in a network. There could be more than one path for power flow but it would travel along the shortest path or lines with less reactance and it is determined as the geodesic path. The adjacency matrix given in equation (1) is used for further analysis and, it is based on the connection diagram of the 30-bus system.

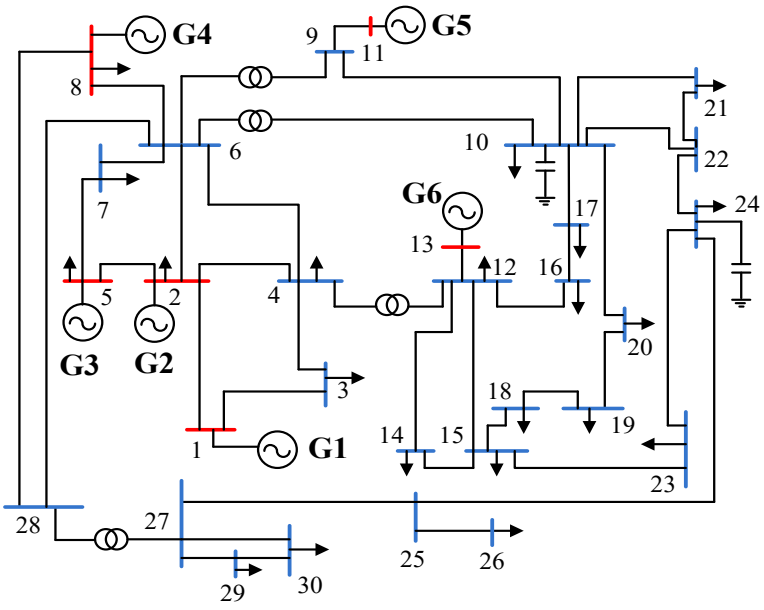

FIGURE 1. IEEE 30 bus system

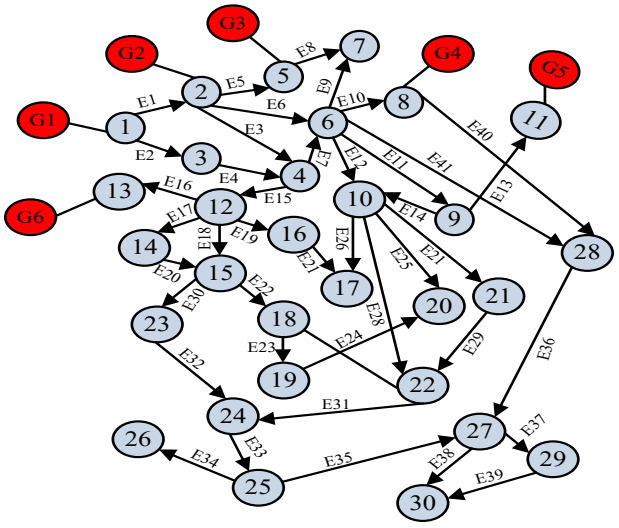

FIGURE 2. Graph theory of 30 bus system

IMPLEMENTATION OF GRAPH THEORY APPROACH ON IEEE 30 BUS SYSTEM

The graph of the 30-bus system is shown in Figure 2 which is considered for the matrix formation according to connectivity. The adjunct matrix from the graph network is given in equation (1),

$$Aij = \begin{bmatrix} a_{1,1} & a_{1,2} & a_{1,3} & a_{1,4} & \cdots & a_{1,n} \\ a_{2,1} & a_{2,2} & a_{2,3} & a_{2,4} & \cdots & a_{2,n} \\ a_{3,1} & a_{3,2} & a_{3,3} & a_{3,4} & \cdots & a_{3,n} \\ a_{4,1} & a_{4,2} & a_{4,3} & a_{4,4} & \cdots & a_{4,n} \\ \cdot & \cdot & \cdot & \cdot & \cdots & \cdot \\ \cdot & \cdot & \cdot & \cdot & \cdots & \cdot \\ \cdot & \cdot & \cdot & \cdot & \cdots & \cdot \\ a_{m,1} & a_{m,2} & a_{m,3} & a_{m,4} & \cdots & a_{m,n} \end{bmatrix} \quad (1)$$

Where A_{ij} is the connection between two vertices i and j.

$$A_{ij} = \left[Line_{ij}^{n}\right] = \begin{cases} 1 & when\ i\ is\ connected\ to\ j \\ 0 & when\ i\ is\ not\ connected\ to\ j \end{cases} \quad (2)$$

At the same time, we consider the reactance of the transmission line as a weighting factor. As the focus of this paper is the impact of the low inertia constant which requires the implementation of a swing equation in a 30-bus system.

The swing equation of the power system is

$$M\frac{d^2}{dt^2}\Delta\delta = P_m - P_e = \Delta P \quad (3)$$

Where δ denotes the rotor angle

M is inertia constant

$$M = J\omega_m \quad (4)$$

Where, J is the total moment of inertia kg-m^2 and ω_m is rotor angular speed, D is the damping constant, P_m and P_e are mechanical and electrical power respectively.

For stability studies the machine data supplied is in terms of inertia constant H;

The inertia constant H is given as

$$H = \frac{Kinetic\ energy\ stored\ in\ joules\ at\ synchronus\ speed}{machine\ rating\ in\ MVA} \quad \frac{\frac{1}{2}J\omega_m^2}{s}MJ/MVA \quad (5)$$

The relationship between M and H,

$$H = \frac{\frac{1}{2}M\omega_m}{S}MJ/MVA \quad (6)$$

and

$$M = \frac{2H}{\omega_m}S\left(MJ/Mech\quad rad\right) \quad (7)$$

The final swing equation for further analysis in terms of H is as follows

$$\frac{2H}{\omega_s}\frac{d^2\delta}{dt^2} = P_m - P_e = \Delta P \quad (8)$$

When generation and demand imbalances; the frequency deviation and RoCoF are given as

$$\omega = \frac{d}{dt}\Delta\delta \quad (9)$$

And

$$\dot{\omega} = \frac{d^2}{dt^2}\Delta\delta \quad (10)$$

Where the RoCoF is derivative of the change in frequency. While applying the swing equation to the system with multiple generators and lines, the network topology must be considered and it is expressed by the graph Laplacian matrix (L).

$$[L]_{n\times n} = [D]_{n\times n} - [A]_{n\times n} \quad (11)$$

Where, D is the diagonal matrix given in equation (12) which depicts the node degree i.e., the number of nodes connected to respective nodes, and A is an adjunct matrix.

$$D = \begin{bmatrix} D_{1,2}+D_{1,3}+D_{1,4}+\cdots+D_{1,n} & 0 & 0 & 0 & \cdots & 0 \\ 0 & D_{2,1}+D_{2,3}+D_{2,4}+\cdots+D_{2,n} & 0 & 0 & \cdots & 0 \\ 0 & 0 & D_{3,1}+D_{3,2}+D_{3,4}+\cdots+D_{3,n} & 0 & \cdots & 0 \\ 0 & 0 & 0 & D_{4,1}+D_{4,2}+D_{4,3}+\cdots+D_{4,n} & \cdots & 0 \\ \cdot & \cdot & \cdot & \cdot & \cdots & \cdot \\ \cdot & \cdot & \cdot & \cdot & \cdots & \cdot \\ \cdot & \cdot & \cdot & \cdot & \cdots & \cdot \\ 0 & 0 & 0 & 0 & \cdots & D_{n,1}+D_{n,2}+D_{n,3}+\cdots+D_{n,n-1} \end{bmatrix} \quad (12)$$

The swing equation describes the rotor dynamics of the synchronous generators and determines the power system stability at various operating conditions. For the frequency stability analysis of the 30-bus system with different generator mixes, the swing equation on each bus is implemented by using the Laplacian matrix (L). The approximated power flow in the network is given in

equation (13) and the first term shows the network topology (Farmer et al. 2022).

It is clear that the network topology and location of buses affects the RoCoF with respect to bus inertial response time.

$$\overline{p} = L \cdot \overline{\delta} \tag{13}$$

At the time of disturbance, the change in power flow is given as

$$\Delta P = L \cdot \overline{\delta_0} - \overline{P_c} \tag{14}$$

Where P_c is the change in power flow and $L \cdot \overline{\delta_0}$ is the initial steady-state power flow

To calculate the rate of change in frequency the swing equation given in (3) and is rearranged as

$$\dot{\overline{\omega}} = -M^{-1} L \Delta \overline{\delta} - M^{-1} \overline{P_c} \tag{15}$$

When we consider the network topology the RoCoF become

$$\dot{\overline{\omega}} = -[M]^{-1}_{m \times n} [L]_{m \times n} \left[\Delta \overline{\delta}\right]_{m \times 1} - [M]^{-1}_{m \times n} \left[\overline{P_c}\right]_{m \times 1} \tag{16}$$

Where,

$$M_{i,j} = \begin{bmatrix} M_{1,1} & 0 & 0 & 0 & \cdots & 0 \\ 0 & M_{2,2} & 0 & 0 & \cdots & 0 \\ 0 & 0 & M_{3,3} & 0 & \cdots & 0 \\ 0 & 0 & 0 & M_{4,4} & \cdots & 0 \\ \vdots & \vdots & \vdots & \vdots & \cdots & \vdots \\ 0 & 0 & 0 & 0 & \cdots & M_{n,n} \end{bmatrix} \qquad M_{i,j} = M_{i,i}, \; i = j$$

and $M = 2H$

$$\Delta\delta = \begin{bmatrix} \Delta\delta_1 \\ \Delta\delta_2 \\ \Delta\delta_3 \\ . \\ . \\ . \\ \Delta\delta_n \end{bmatrix} \quad \text{and} \quad P_c = \begin{bmatrix} \Delta P_1 \\ \Delta P_2 \\ \Delta P_3 \\ . \\ . \\ . \\ \Delta P_n \end{bmatrix}$$

Where, H is the inertia constant of the respective bus. The first term in equation (16) considers the power flow together with the inertia locations through the network Laplacian. The network Laplacian contains topological information which describes the power flow path in the network. The disturbance size and location are represented by the vector P_c.

TABLE 1. Case 1 - 4 are a combination of the generating resources in the IEEE 30 bus system

Generator bus	Case 1	Case 2	Case 3	Case 4
1	Thermal	Solar	Thermal	Solar
2	Thermal	Thermal	Solar	Solar
5	Hydro	Hydro	Hydro	Hydro
8	Solar	Thermal	Thermal	Thermal
11	Wind	Wind	Wind	Wind
13	Solar	Thermal	Thermal	Thermal

ANALYSIS OF THE EFFECT OF GENERATION MIXES AND THEIR LOCATION ON INERTIA CONSTANT IN POWER SYSTEM

The location of vertices in the graph and the type of generator connected to it are responsible for the RoCoF performance at other nodes of the network.

This is demonstrated by varying the location of the generator type connected to the node or vertices. The different cases considered for this analysis are elaborated in table 1. In IEEE 30 bus system, the generator connected nodes are 1,2,5,8,11, and 13 respectively. Case 1 – case 4 represents the diverse combination of the generation mixes in the 30-bus system. RES especially solar PV generators connected node contains lesser inertia as compared to other nodes. The low inertia nodes with a higher degree of connection can be catastrophic in the system for any small disturbances.

This paper explores, the pathfinding algorithm for graph theory implemented on the IEEE 30-bus system. The pathfinding algorithm investigates the shortest path between the nodes.

From this information on the path length from the source node, it is possible to find the impact of the low inertia node on the system. The placement of the RES must

not affect the stable operation of the power grid while considering this the different cases are shown in Table 1 are analyzed in figures 3 and 4 respectively.

In case 1, the thermal generator is placed at the node 1 and 2, and the solar generation system with very least inertia constant is placed at 8 and 13. As nodes 1 and 2 are connected to the maximum number of nodes and they contains higher a inertia constant among all so the system is more stable in nature in case 1, according to the RoCoF value of the nodes depicted in figure 3. The placement of solar generation at both dominating nodes 1 and 2 in case number 4 is showing the worst performance of RoCoF as compared with other cases. In case 4 almost all nodes violate the tolerance limit of RoCoF and Frequency nadir. This comparison of the cases is clearly given in table 2.

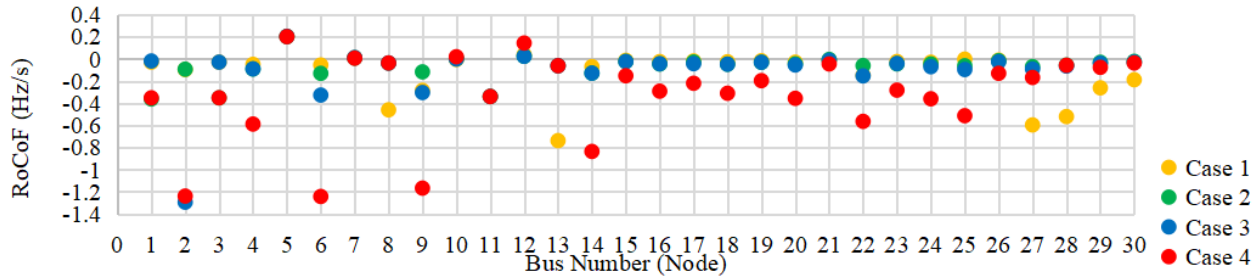

FIGURE 3. Rate of change of frequency at nodes of 30 bus system during generation mixes

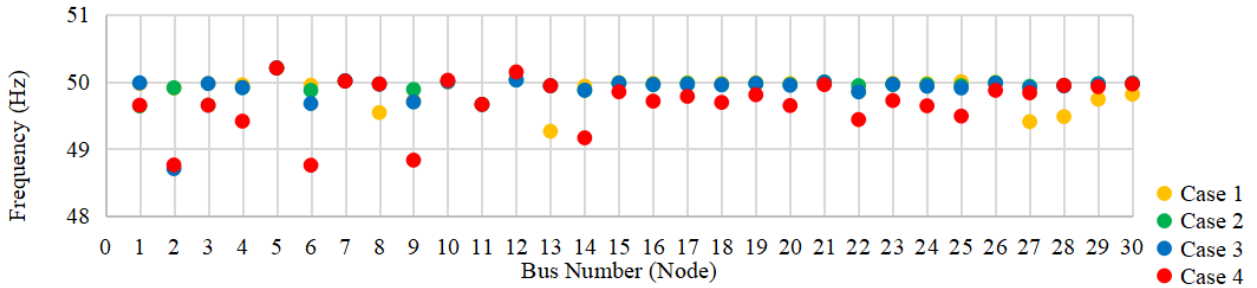

FIGURE 4. Frequency nadir at nodes of 30 bus system during generation mixes

TABLE 2. Frequency response analysis of the impact of generation mixes and their location in the network

Node	Case 1		Case 2		Case 3		Case 4	
	RoCoF	Frequency Nadir	RoCoF	Frequency Nadir	RoCoF	Frequency Nadir	RoCoF	Frequency Nadir
1	-0.0333	49.9667	-0.4	49.6	-0.0333	49.9666	-0.4000	49.6
2	-0.1107	49.8893	-0.1107	49.8892	**-1.3287**	**48.6713**	**-1.3287**	**48.6713**
3	-0.0296	49.9703	-0.3561	49.6439	-0.0297	49.9703	-0.3561	49.6439
4	-0.0575	49.9425	-0.1062	49.8938	-0.1062	49.8938	**-0.6903**	**49.3096**
5	0.1906	50.1906	0.1906	50.1906	0.1906	50.1906	0.1906	50.1906
6	-0.1203	49.8797	-0.1560	49.8439	-0.3849	49.6150	**-1.4435**	**48.5564**
7	0.0033	50.0032	0.0023	50.0023	0.0037	50.0037	0.0019	50.0019
8	**-0.5084**	**49.4916**	-0.0423	49.9576	-0.0423	49.9576	-0.0424	49.9576
9	-0.3104	49.6896	-0.1342	49.8657	-0.3311	49.6689	**-1.2416**	**48.7584**
10	-0.0543	49.9457	-0.0234	49.9765	-0.0579	49.9420	-0.2172	49.7828
11	-0.3500	49.6499	-0.3500	49.6499	-0.3500	49.6499	-0.3500	49.6499
12	-0.0023	49.9977	-0.0042	49.9958	-0.0042	49.9958	-0.0272	49.9728

continue ...

... cont.

13	**-0.7662**	**49.2338**	-0.0638	49.9361	-0.0638	49.9361	-0.06385	49.9361
14	-0.0773	49.9227	-0.1426	49.8573	-0.1426	49.8573	**-0.9272**	**49.0728**
15	-0.0252	49.9748	-0.0464	49.9535	-0.0465	49.9535	-0.3020	49.6979
16	-0.0308	49.9692	-0.0568	49.9431	-0.0568	49.9431	-0.3697	49.6302
17	-0.0230	49.9770	-0.0349	49.9650	-0.0538	49.9462	-0.2755	49.7244
18	-0.0316	49.9684	-0.0584	49.9416	-0.0584	49.9416	-0.3797	49.6203
19	-0.0196	49.9803	-0.0363	49.9637	-0.0363	49.9637	-0.2358	49.7641
20	-0.0343	49.9657	-0.0522	49.9477	-0.0632	49.9367	-0.4114	49.5886
21	-0.0162	49.9837	-0.0070	49.9930	-0.0173	49.9826	-0.0649	49.9350
22	-0.1586	49.8413	-0.0686	49.9314	-0.1692	49.8307	**-0.6347**	**49.3653**
23	-0.0314	49.9686	-0.0579	49.9420	-0.0579	49.9420	-0.3764	49.6236
24	-0.0429	49.9570	-0.0655	49.9345	-0.1006	49.8993	**-0.5158**	**49.4842**
25	-0.0554	49.9445	-0.0845	49.9154	-0.1299	49.8700	**-0.6658**	**49.3347**
26	-0.0171	49.9828	-0.0262	49.9738	-0.0402	49.9598	-0.2060	49.7940
27	**-0.9209**	**49.0791**	-0.1075	49.8924	-0.1417	49.8583	-0.2456	49.7544
28	**-0.6519**	**49.3480**	-0.0705	49.9295	-0.0828	49.9172	-0.0852	49.9147
29	-0.4350	49.5650	-0.0508	49.9491	-0.0669	49.9330	-0.1160	49.8839
30	-0.3992	49.6008	-0.0467	49.9532	-0.0614	49.9385	-0.0779	49.9221

According to the above investigation on power system networks with RES by varying their contribution and location, the inertia constant quantity becomes heterogeneous in nature. The 30-bus system with heterogenous inertia constant affects the systems RoCoF and frequency nadir, as the detailed comparison is manifested in table 3. It is clear that case 2 shares 51.28% share of RES without affecting the nodes in the network. Because of this, case 2 is considered for further analysis of the application of the pathfinding algorithm in power systems.

TABLE 3. Affected nodes due to percentage-wise share of the RES and its location in 30 bus system

	Percentage Share of RES	Location of RES (at node number)	Affected Nodes	RoCoF (Hz/s) at affected nodes	Frequency Nadir (Hz) at affected nodes
Case 1	27%	8, 11, 13	8,13,27,28	-0.4600, -0.7382, -0.5964, -0.5208	49.5400, 49.2618, 49.4036, 49.4792
Case 2	51.28%	1,11	-	-	-
Case 3	25.64%	2,11	2	-1.2945	48.7055
Case 4	68.37%	1,2,11	2,6,9,14,22,25	-1.2393, -1.2430, -1.1676, -0.8360, -0.5642, -0.5129	48.7607, 48.7570, 48.8324, 49.1640, 49.4358, 49.4871

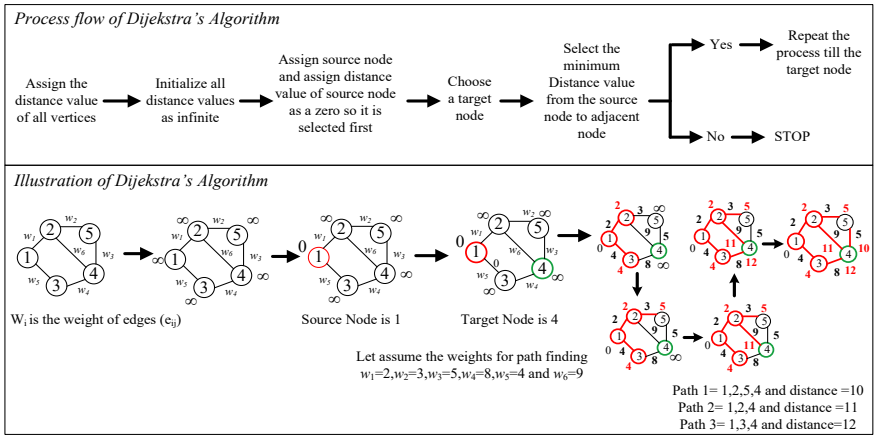

FIGURE 5. Process flow and Illustration of Dijkstra's Algorithm

APPLICATION OF PATHFINDING ALGORITHM (IEEE 30-BUS CASE)

The power system network is converted into graph theory for finding the impact of contingency events in a low inertia grid. As per the discussion in the above section, the location of the generating resources plays an important role to determine the inertia value in the power system. According to this, the network topology offers the impact of inertia value in the system with a share of renewable energy sources. The Laplacian matrices of the system depict the network topology and its connectivity. The nodes are connected through many paths between them, but the power flow follows the path with the least reactance between the nodes. The shortest path between the nodes is determined by the minimum total weight between the two nodes. Here, in the graph theory approach for the power systems, the reactance of the transmission line is considered as the weight of the edges connected between nodes. This section discusses the methodology to determine the vulnerable nodes in a mixed generation power system by using the Dijkstra algorithm.

The nodes which are connected to the generators through the shortest path follow the inertia constant value of the generator connected to the adjacent node. The Dijkstra path-finding algorithm finds the shortest path by calculating the distance between a source node and a target node. The distance between the two nodes is determined by the total weight of the edges connected to the nodes. The algorithm forms a spanning tree as an intermediate step to find the shortest path. The exact elaboration of Dijkstra's algorithm with illustration is given in figure 5. An illustration of the graph with 5 nodes is considered to elaborate the flow of Dijkstra's algorithm. Here, we assume node 1 as the source node and node 4 as the target node. There are total three paths from node 1 to node 4. All three paths with their visited nodes and total weight is shown in figure 5, and out of all three paths the algorithm follows the route with least weight. Though path 1 visited maximum nodes than path 2 and 3, the Dijestra's algorithm gives path 1 as a shortest path because of total edge weight is lesser than other possible paths. This is implemented in IEEE 30 bus system to investigate the vulnerable nodes in the system with the maximum possible contribution of RES. The aforementioned results analysis in table 3 states that case 2 contains the highest share of RES without affecting the RoCoF and frequency nadir limits. Therefore case 2 is considered for the implementation of Dijkstra's algorithm for further analysis. For an example, the disturbance is created at node number 17 and it is counted as the target node. The path followed by Dijkstra's algorithm from the source to the target node is compared with all possible paths in Table 4.

According to the directed graph of the 30-bus system given in Figure 2, the power feed to node 17 is from generator-connected nodes 1 and 2. It is clear from Table 4, the route between connected nodes 2-7 is the shortest with a 0.5788 cost value in comparison with path 1-17. The thermal generator is connected to node number 2 as we know thermal contains a higher inertia value therefore node number 17 can be considered a stable node. Figure 7 depicts the implementation of path finding Dijkstra's algorithm in a connected graph of 30 bus systems. The red edges denote the possible paths from the source to the target node and the green one shows the geodesic path calculated by Dijkstra's algorithm. From this analysis, it is noticed that edge weight and connectivity are playing an important role in graph theory. The common edge in all shortest paths between two nodes shows the betweenness index of the graph.

GRAPH CENTRALITY INDEX

It is observed from the analysis of the application of pathfinding Dijkstra's algorithm, the occurrence of the edge in every possible shortest path is considered as the edge betweenness of the graph. The betweenness centrality is described as the total number of shortest paths going through the particular edge or node. The basic philosophy of the electric circuit always follows the low reactance path and here, edge weight is considered as a transmission line reactance. While considering this, the edge with the least reactance values transfers more power and is treated as the edge with high betweenness index.

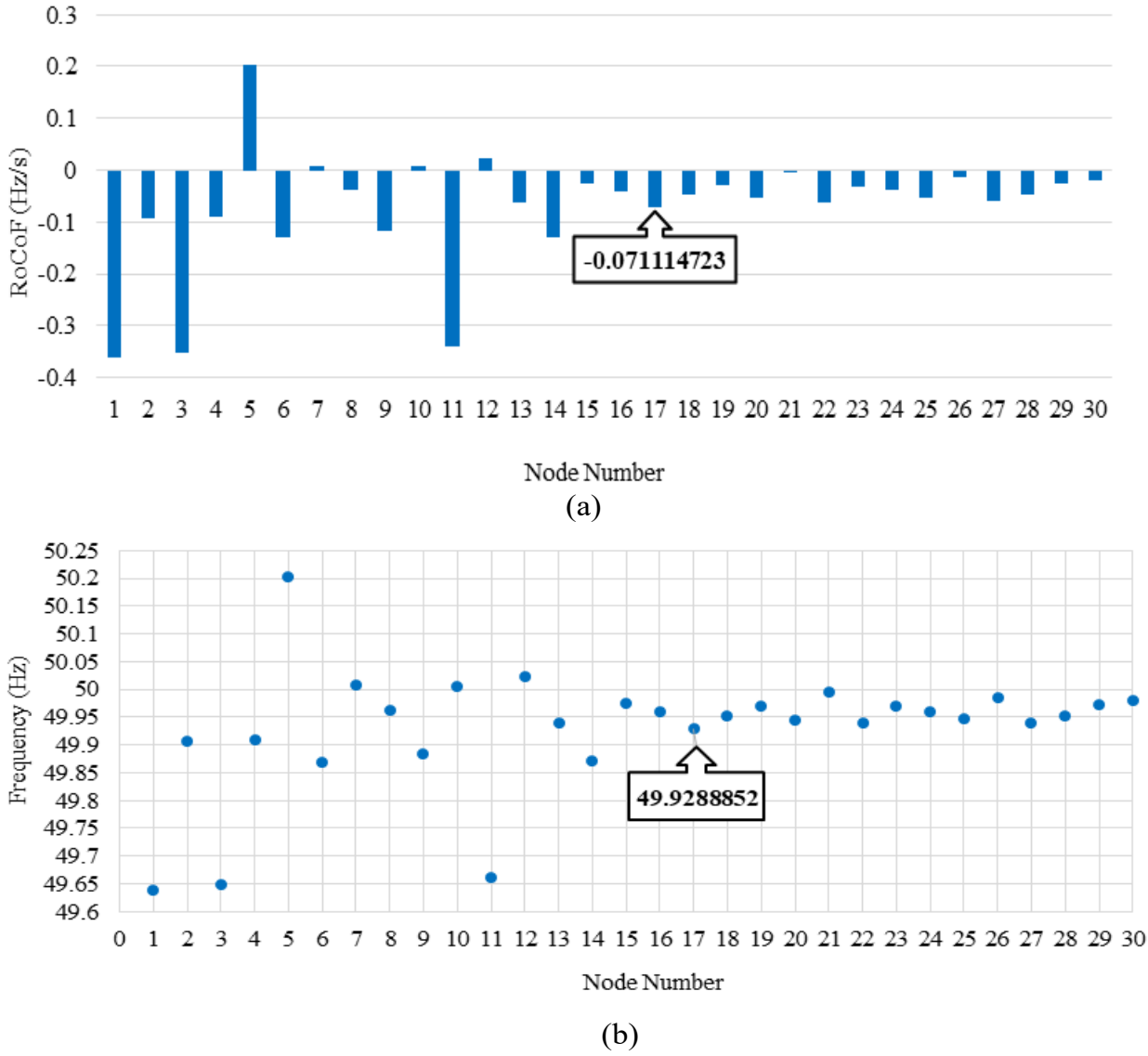

FIGURE 6. Performance of RoCoF (a) and Frequency Nadir (b) at disturbance that occurred on node 17

Figure 8 depicts the edges having a high line betweenness centrality value from source node 1 in (a) and node 2 in (b). It is observed that an edge betweenness index varies as the source node changes. The effect of inertia constant value depends on the node centrality. The nodes connected to the edges with high betweenness index may have a high centrality value. The node centrality is again distributed in degree and betweenness centrality.

TABLE 4. Application of Dijkstra's algorithm and comparison with other possible paths

Connected node	Number of possible Paths	Paths	Cost	Dijkstra's Algorithm Path	Dijkstra's Algorithm Cost
		Perturbed Node 17			
1 - 17	5	1,3,4,12,16,17	0.8710	1,3,4,6,9,10,17	0.6670
		1,2,4,12,16,17	0.8791		
		1,3,4,6,10,17	0.905		
		1,2,4,6,10,17	0.9131		
		1,3,4,6,9,10,17	0.667		

continue ...

2 - 17	4	2,4,6,10,17	0.8556	2,6,9,10,17	0.5788
		2,6,10,17	0.8168		
		2,4,12,16,17	0.8216		
		2,6,9,10,17	0.5788		

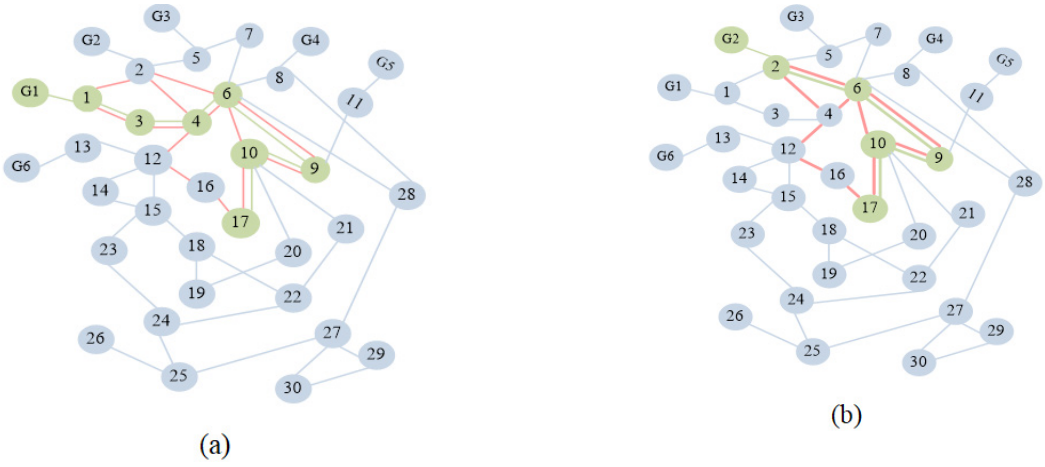

(a) (b)

FIGURE 7: Dijkstra's algorithm shortest path from 1-17 in (a) and 2-17 in (b)

1. Degree Centrality is the ranking of the nodes with more connections, for a directed graph the degree centrality is given as

$$Degree\ centrality(C_D) = \frac{Out\ Degree}{Total\ number\ of\ nodes - 1} \quad (17)$$

Node numbers 6,10,12 have a high degree centrality as shown in figure 9. The connectivity of these nodes is higher than other nodes and if these are low inertia nodes then it can affect the system's maximum nodes with a higher RoCoF rate.

2. Betweeness centrality is the maximum occurrence of the node in the shortest paths between the source and remaining nodes of the graph.

$$Betweeness\ Centrality\ (C_B) = \frac{\sum P_{ij}(k)}{P_{ij}} \quad (18)$$

Where, P_{ij} is the shortest path between node i and j, and k is the maximum occurrence of the node. The pathfinding algorithm given by Dijkstra mentioned in section 3 is used to determine the shortest path to detect the betweenness centrality of the node. The difference between degree and betweenness centrality is clearly observed in figures 9 and 10. In the case of degree centrality value node 6, 10, and 12 have higher centrality, and in the case of betweenness centrality node 6 have higher centrality among all. Further analysis is to verify the centrality of a graph in the next section. The verification is done by varying the load connected (or creating the disturbance) to the respective bus to check which centrality value is useful to find the vulnerable nodes in a low inertia power system.

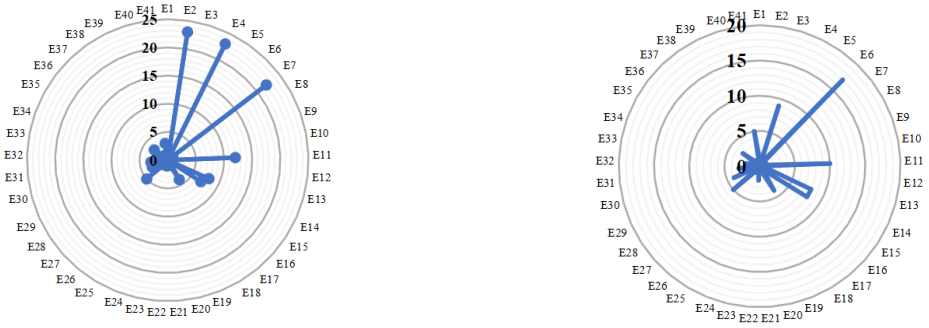

(a) (b)

FIGURE 8. line betweenness of 30 bus system from source node 1 in (a) and node 2 in (b)

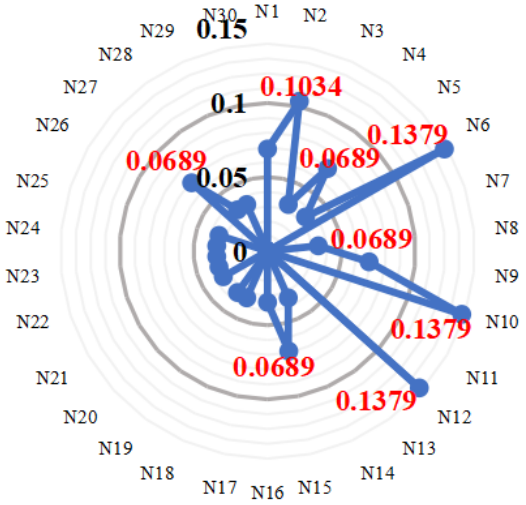

FIGURE 9. Degree centrality of node

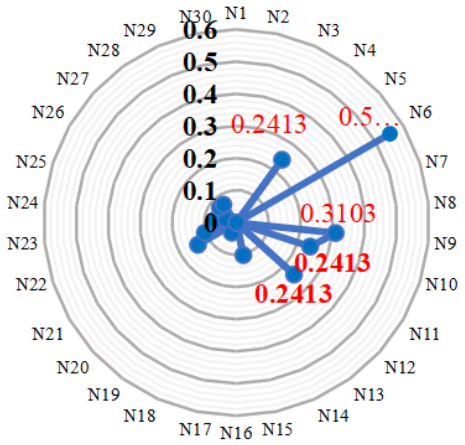

FIGURE 10. Betweenness centrality of node

ANALYSIS OF THE EFFECT OF CHANGE IN LOAD ON THE 30-BUS SYSTEM WITH A CONTRIBUTION OF RES

The aforementioned analysis of the 30-bus system with a contribution of renewable energy sources on frequency response is studied in section 2. The maximum possible RES integration (51.28%) in 30 bus system without violating the RoCoF limit is demonstrated in case 2. Therefore, it is taken to examine the effect of load variation and vulnerable nodes in the 30-bus system connected with the maximum possible RES. The other cases described in section 2.2 are avoided because they have reached the lower frequency nadir at some nodes due to low inertia and the unsuitable location of RES in view of the dynamic stability of the system.

FREQUENCY RESPONSE ANALYSIS BY PERTURBING NODE WITH HIGH ROCOF

The nodes with maximum frequency nadir are 1, 3, 11,6,9,14, and 27 (refer to case 2 in table 2) respectively out of these nodes 3 and 14 are perturbed with a step change in the load of 0.1 pu.

In figures 11 and 12, the perturbed node with higher RoCoF shows the maximum deviation in frequency nadir. According to their higher RoCoF value, these nodes contain lower inertia and violets an acceptable range of frequency. The other nodes are not affected because their centrality value is almost zero. From the RoCoF point of view, these nodes can be considered vulnerable and require inertial power for the occurrence of any small variation of power.

From the above figures 11 and 12, the perturbed node with higher RoCoF shows the maximum deviation in frequency nadir. According to their higher RoCoF value, these nodes contain lower inertia and violets an acceptable range of frequency. The other nodes are not affected due to the centrality value of these nodes being almost zero. From the RoCoF point of view, these nodes can be considered vulnerable and require inertial power for the occurrence of any small variation of power.

FREQUENCY RESPONSE ANALYSIS OF PERTURBING THE NODE WITH THE HIGHEST CENTRALITY VALUE

The higher degree centrality nodes are 6,10,12 with values of 0.14 respectively, and node 6 with the highest betweenness centrality value is 0.5517. After perturbing nodes 6 and 10 the affected nodes are depicted in figures 13 and 14. It clarifies that node number 6 with high betweenness index affects more nodes. According to this observation, it can be concluded that the betweenness centrality plays an important role to find vulnerable nodes from the highest connectivity point of view. The pathfinding algorithm given by Dijkstra is used to determine the betweenness centrality of the node. The critical analysis of the graph theory approach to find the effect of low inertia on the system is given in table 5. The node with low inertia than usual and also have high a betweenness index that can be considered as the most vulnerable

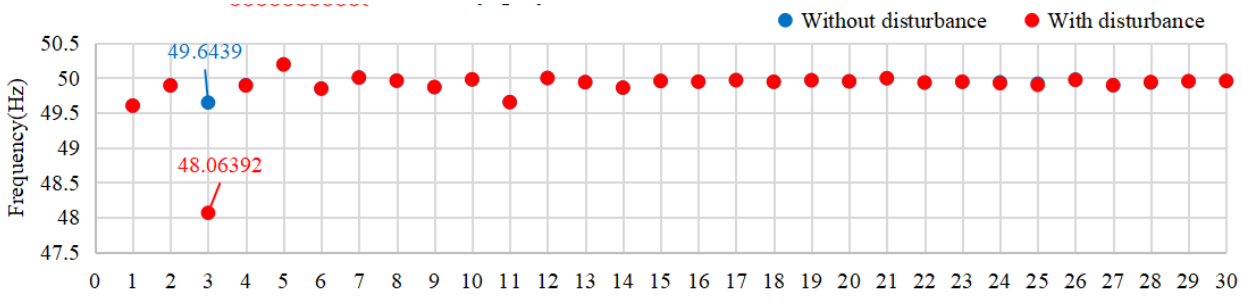

FIGURE 11 Frequency at node 3 after perturbation

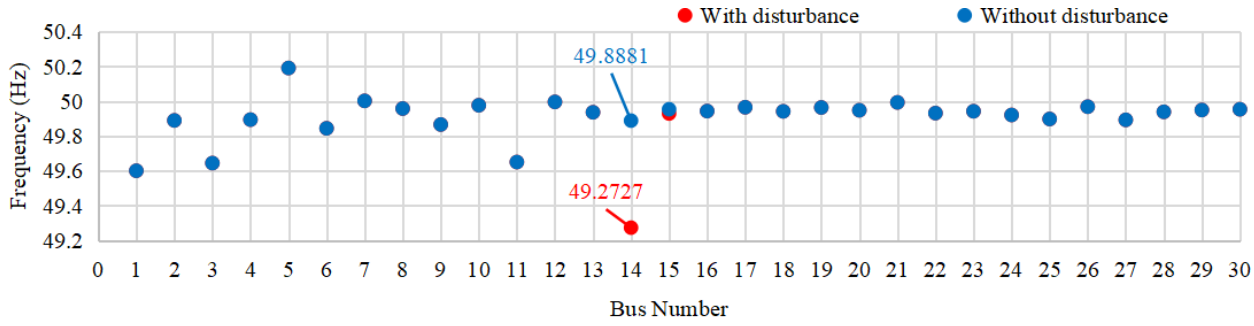

FIGURE 12. Frequency at node 14 after perturbation

nodes of the system. The node connected to source node with a higher inertia constant through the shortest path and also with less centrality is counted as a stable node in the system (for eg. Node 17 given in Table 5).

An effect of node centrality is described in section 4, the higher centrality value (figures 9 and 10) maximum node will get affected after perturbing respective nodes (figures 13 and 14). The number of nodes affected are more in figure 13 because it follows the occurrence of node in the shortest path from the source node. Node number 6 has the highest degree and betweenness centrality too but node number 10 has only a higher degree centrality. Figure 13 and 14 clarifies that betweenness centrality must be considered for the effect of heterogenous inertia in the mixed generation systems. Table number 5 gives the numerical analysis of frequency at nodes with inertia constant value and from this, we can predict the requirement of inertial power at a particular node (bus). The nodes highlighted with orange color violate the maximum permissible limit of the acceptable frequency band at small perturbations. It needs more inertial power, to maintain the frequency during normal power system operation. The nodes highlighted with yellow color have frequency deviation on the verge of an acceptable limit but still, it requires inertial power to maintain the frequency at large disturbances.

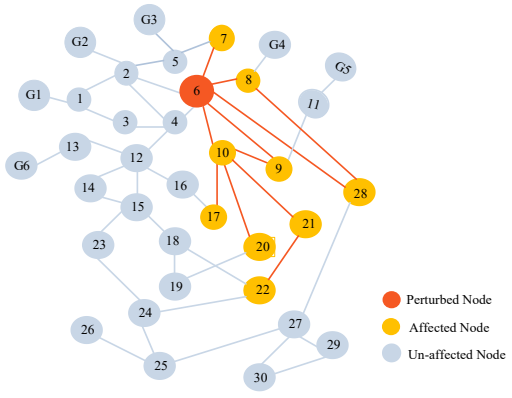

FIGURE 13. Affected nodes due to perturbation at node 6

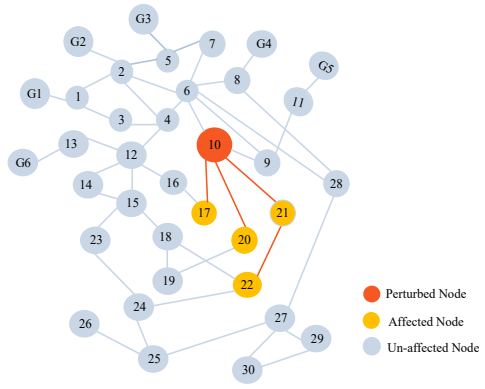

FIGURE 14. Affected nodes due to perturbation at node 10

TABLE 5. Detailed analysis of frequency response at various scenarios in 30-bus system to identify the vulnerable nodes

Disturbed Node	Affected Nodes	RoCoF (Hz/s)		Frequency (Hz)		Inertia constant H(s)
		Pre-disturbance	Post-disturbance	Pre-disturbance	Post-disturbance	
Node 3	3	-0.3561	-1.9361	49.6439	48.06392	0.5000
Node 6	6	-0.1561	-0.4615	49.8439	49.5385	4.6250
	7	0.0023	-0.0053	50.0023	49.9946	4.6250
	8	-0.0423	-0.0452	49.9576	49.9548	6.0000
	9	-0.1342	-0.1522	49.8657	49.8477	4.6250
	10	-0.0234	-0.1009	49.9765	49.8991	4.6250
	17	-0.0349	-0.0414	49.9650	49.9585	3.9375
	20	-0.0522	-0.0682	49.9477	49.9318	3.9375
	21	-0.0070	-0.0119	49.9930	49.9881	4.6250
	22	-0.0686	-0.0783	49.9314	49.9216	4.6250
	28	-0.0705	-0.0659	49.9295	49.9341	5.3125
Node 10	10	-0.0235	-0.1364	49.9765	49.8635	4.6250
	17	-0.0349	-0.0436	49.9650	49.9564	3.9375
	20	-0.0522	-0.0735	49.9477	49.9265	3.9375
	21	-0.0070	-0.0135	49.9929	49.9865	4.6250
	22	-0.0686	-0.0816	49.9313	49.9184	4.6250
Node 14	14	-0.1426	-0.7272	49.8573	49.2727	3.2500
Node 15	15	-0.0465	-0.2618	49.9535	49.73815	3.2500
	18	-0.0584	-0.0853	49.9416	49.91469	3.9375
	23	-0.0407	-0.0582	49.9593	49.94184	4.6250
Node 17	17	-0.0349	-0.0711	49.9650	49.9289	3.9375

CONCLUSION

In real power system operation, the RoCoF relays disconnect the generators when its violets the RoCoF limits. The future power network with a maximum contribution of RES will create low inertia in the grid and it is responsible to limit high RoCoF after the first few seconds of disturbance. The investigation of the impact of heterogenous inertia on the system is done in this paper. The graph theory approach is used to determine the affected or vulnerable nodes due to the impact of low inertia on the system. The network topology plays an important role to determine the effect of location and share of RES on the frequency response of the system. It is justified in an analysis of 30 bus system graph theory by applying the pathfinding algorithm and node centrality index. It is difficult to manage frequency regulation in the network with heterogeneously distributed inertia constant. This issue can be resolved by investigating node-wise RoCoF value at various power system operating conditions. Dijkstra's algorithm is used to find the shortest path between the nodes and also used to find the betweenness centrality of the node. It is concluded that the betweenness centrality plays an important role to find the vulnerable and affected nodes. It is demonstrated by creating the disturbance at node number 6 and node number 10, both nodes have the same degree centrality but node number 6 has higher betweenness centrality and it affects more nodes in the system. If the disturbance occurs at a vulnerable node with a very low inertia constant, then it can be a catastrophic phenomenon in the power system. It is concluded that the geodesic distance between generating and destination nodes as well as the betweenness centrality of a node can be used to find the impact of low inertia in future power system planning.

ACKNOWLEDGEMENT

We would to thank Sardar Vallabhbhai National Institute of Technology, Gujrat, India for supporting this study.

DECLARATION OF COMPETING INTEREST

None

REFERENCES

Alahmad, B. 2021. *The Role of Location of Low Inertia in Power Systems*. Generic.

Azizi, S., Sun, M., Liu, G. &Terzija, V. 2020. Local frequency-based estimation of the rate of change of frequency of the center of inertia. *IEEE Transactions on Power Systems* 35: 4948-4951.

Basri, S., Zakaria, S. U., Kamarudina & Siti Kartom. 2021. Review on alternative energy education in Malaysia.2021. *Jurnal Kejuruteraan* 33: 461-472.

Brahma, D. & Senroy, N. 2021. Spatial distribution of grid inertia and dynamic flexibility: Approximations and applications. *IEEE* 36: 3465-3474.

Denholm, P., Mai, T., Kenyon, R. W., Kroposki, B. & O'Malley, M. 2020. Inertia and the power grid: A guide without the spin, 2020, National Renewable Energy Lab. (NREL), Golden, CO (United States).

Dwivedi, Ajendra., Yu, Xinghuo & Sokolowski, Peter. 2009. Identifying vulnerable lines in a power network using complex network theory. *IEEE International Symposium on Industrial Electronics*: 18-23.

Entsoe, Inertia, and rate of change of frequency (RoCoF). Version 17.2020.

Farmer, Warren J., Rix & Arnold, J. 2022. Evaluating power system network inertia using spectral clustering to define local area stability. *International Journal of Electrical Power & Energy Systems* 134: 107404.

Garg, R. K., Agrawal, V. P. & Gupta, V. K. 2006. Selection of power plants by evaluation and comparison using graph theoretical methodology. *International Journal of Electrical Power & Energy Systems* 28: 429-435.

Harun, Li Yang & Irina. 2022. Renewable energy scenarios for sustainable electricity in malaysia and the application of Analytical Hierarchy Process (AHP) for Decision-making. *Jurnal Kejuruteraan* 34: 1271-1279.

Iyer, MCC., Shivkumar, V., Belur & Madhu, N. 2010. Application of graph theory in stability analysis of meshed microgrids. Proceedings of the 19th International Symposium on Mathematical Theory of Networks and Systems–MTNS. 2010.

Kerdphol, T., A. Rahman, Fathin S. & Mitani, Y. 2018. Virtual inertia control application to enhance frequency stability of interconnected power systems with high renewable energy penetration. *Energies* 11: 981.

Makolo, P., Zamora, R. & Lie, T. 2021. Online inertia estimation for power systems with high penetration of RES using recursive parameters estimation. *IET Renewable Power Generation* 15: 2571-2585.

Mandal, R. & Chatterjee, K. 2021. Virtual inertia emulation and RoCoF control of a microgrid with high renewable power penetration. *Power Systems Research* 194: 107093.

Mehigan, L., Al Kez, D., Collins, S., Foley, A., Ó'Gallachóir, B. & Deane, P. 2020. Renewables in the European power system and the impact on system rotational inertia. 203: 117776.

Mudaheranwa, E., Sonder, Hassan B.,Cipcigan, L. & Ugalde-Loo, C E. 2022. Estimation of Rwanda's power system inertia as input for long-term dynamic frequency response regulation planning. *Electric Power Systems Research* 207: 107853.

Nerkar, H., Kundu, P. & Chowdhury, A. 2023. An analysis of the impact on frequency response with penetration of RES in power system and modified virtual inertia controller. *Journal of Operation and Automation in Power Engineering* 11: 39-49.

Nerkar, H., Kundu, P. & Choudhury, A. 2021. Frequency control ancillary services in power system with integration of PV generation. 2021 International Conference on Intelligent Technologies (CONIT). p.1-6. IEEE.

Nouti, D., Ponci, F. & Monti, A. 2021. Heterogeneous Inertia Estimation for Power Systems with High Penetration of Converter-Interfaced Generation. *Energies* 14: 5047.

Pentayya, P., Verma, UK., Mukhopadhyay, P., Mitra, G., Bannerjee, S., Thakur, M. & Sahay, S. Adaptive df/dt Relay-A case study with reference to the Indian Power System. Journal Article.

Prabhakar, K., Jain, Sachin K. & Padhy, P.K. 2022. Inertia estimation in modern power system: A comprehensive review. *Electric Power Systems Research* 211: 108222. Elsevier.

Phurailatpam, C., Rather, Z.H., Bahrani, B. & Doolla, S. 2021. Estimation of non-synchronous inertia in AC microgrids. *IEEE* 12: 1903-1914.

POSOCO, IITB. 2022. Report on assessment of inertia in Indian power system.

Qaid, K., Gan, C., Salim, N. & Ibrahim, K. 2021. Effects of generator ratings on inertia and frequency response in power systems. *IOP Conference Series: Materials Science and Engineering* 1127: 012034.

Rampokanyo, M. & Ijumba-Kamera, P. 2019. Power system inertia in an inverter-dominated network. *Journal of Energy in Southern Africa* 30: 80-86.

Rezkalla, M., Pertl, M. & Marinelli, M. 2018. Electric power system inertia: Requirements, challenges and solutions. *Electrical Engineering*100: 2677-2693.

Retiére, N., Ha, D. & Caputo, J. 2019. Spectral graph analysis of the geometry of power flows in transmission networks. *IEEE Systems Journal* 14: 2736-2747.

Shahidehpour, M. & Wang, Y. 2004. *Communication And Control in Electric Power Systems: Applications of Parallel and Distributed Processing*. John Wiley & Sons.

Su, Y.,Li, H., Cui, Y.,You, S., Ma, Y., Wang, J. & Liu, Y. 2022. An adaptive pv frequency control strategy based on real-time inertia estimation. *IEEE Transactions on Smart Grid* 12: 2355-2364.

Tamrakar, U., Shrestha, D., Maharjan, M., Bhattarai, Bishnu P., Hansen, T. & Tonkoski, R. 2017. Virtual inertia: Current trends and future directions. *Applied Sciences* 7: 654.

Tan, B., Zhao, J., Netto, M., Krishnan, V., Terzija, V. & Zhang, Y. 2022. Power system inertia estimation: Review of methods and the impacts of converter-interfaced generations. *International Journal of Electrical Power & Energy Systems* 134: 107362.

Wilson, D., Yu, J., Al-Ashwal, N., Heimisson, B. & Terzija, V. 2019. Measuring effective area inertia to determine fast-acting frequency response requirements. *International Journal of Electrical Power & Energy Systems* 113: 1-8.

Wu, Y. & Huang, C. 2021. Estimation of power system inertia-A case study in Taiwan. IEEE International Future Energy Electronics Conference (IFEEC). p.1-6. IEEE.